J Biol Phys (2007) 33:399–419
DOI 10.1007/s10867-008-9058-3

ORIGINAL PAPER

Analytical Ultracentrifugation Sedimentation Velocity for the Characterization of Detergent-Solubilized Membrane Proteins Ca^{++}-ATPase and ExbB

Andrés G. Salvay · Monica Santamaria · Marc le Maire · Christine Ebel

Received: 23 October 2007 / Accepted: 28 January 2008 /
Published online: 25 April 2008

Abstract We have investigated the potential of new methods of analysis of sedimentation velocity (SV) analytical ultracentrifugation (AUC) for the characterization of detergent-solubilized membrane proteins. We analyze the membrane proteins Ca^{++}-ATPase and ExbB

A. G. Salvay · C. Ebel (✉)
CNRS, IBS, Laboratoire de Biophysique Moléculaire, 41 rue Jules Horowitz, Grenoble 38027, France
e-mail: christine.ebel@ibs.fr

A. G. Salvay · C. Ebel
CEA, DSV, IBS, Grenoble 38027, France

A. G. Salvay · C. Ebel
Université Joseph Fourier, Grenoble 38000, France

A. G. Salvay
Instituto de Física de Líquidos y Sistemas Biológicos, Universidad Nacional de La Plata, c.c. 565, B1900BTE La Plata, Argentina

A. G. Salvay
Departamento de Ciencia y Tecnología, Universidad Nacional de Quilmes, Roque Sáenz Peña 352, B1876BXD Bernal, Argentina

M. Santamaria
IBBMC, Université de Paris-Sud, Orsay, France

M. le Maire
CEA, iBiTecS, Service de Bioénergétique Biologie Structurale et Mécanismes, Laboratoire Proteines membranaires, Gif sur Yvette cedex 91191, France

M. le Maire
CNRS, URA 2096, Gif sur Yvette cedex 91191, France

M. le Maire
Université Paris-Sud 11, LRA17V Gif sur Yvette cedex 91191, France

Present address:
M. Santamaria
Division de Hepatologia y Terapia Genica, CIMA—Universidad de Navarra, 31080 Pamplona, España

solubilized with DDM (dodecyl-β-D-maltoside). SV is extremely well suited for characterizing sample heterogeneity. DDM micelles (s_{20w}=3.1 S) and complexes (Ca^{++}-ATPase: s_{20w}=7.3 S; ExbB: s_{20w}=4 S) are easily distinguished. Using different detergent and protein concentrations, SV does not detect any evidence of self-association for the two proteins. An estimate of bound detergent of 0.9 g/g for Ca^{++}-ATPase and 1.5 g/g for ExbB is obtained from the combined analysis of SV profiles obtained using absorbance and interference optics. Combining s_{20w} with values of the hydrodynamic radius, R_s=5.5 nm for Ca^{++}-ATPase or R_s=3.4 nm for ExbB, allows the determination of buoyant molar masses, M_b. In view of their M_b and composition, Ca^{++}-ATPase and ExbB are monomers in our experimental conditions. We conclude that one of the main advantages of SV versus other techniques is the possibility to ascertain the homogeneity of the samples and to focus on a given complex even in the presence of other impurities or aggregates. The relative rapidity of SV measurements also allows experiments on unstable samples.

Keywords Analytical ultracentrifugation · Membrane proteins · Ca^{++}-ATPase · ExbB

1 Introduction

Membrane proteins perform a wide range of essential cellular functions. Pores, channels, pumps, and transporters control the transport of ions and metabolites between the cell and the extracellular environment or between cellular compartments. Photosynthetic proteins and respiratory enzymes allow the conversion of energy into a form useful for the cell. Signal transduction involves receptors that sense changes in the cellular environment, e.g., differences in hormones, light, or mechanical stimulation, to initiate specific cell responses. Membrane proteins are involved in a number of genetic diseases and have considerable therapeutic importance: half of drug targets are membrane receptors or ion channels.

The characterization of the interactions and structures of membrane proteins is often difficult based on their low natural abundance, their low overexpression rate, and their difficult extraction from their natural lipid environment. The number of available structures is increasing rapidly, but few membrane protein structures are still known as compared with soluble proteins (http://blanco.biomol.uci.edu/Membrane_Proteins_xtal.html).

Detergents are most commonly used to solubilize, stabilize, and manipulate membrane proteins for the characterization of their function and structure. Different environments such as amphipatic polymers have been also successfully investigated for their stabilization in solution [1, 2]. The stability and composition of the protein–detergent complexes depend on the type and concentration of the detergent [3–6]. When decreasing the detergent concentration below, or even slightly above, the critical micelle concentration (CMC, the minimum concentration to form micelles), membrane proteins aggregate and precipitate. Above the CMC, the detergent is bound in quantities that are highly variable and can be very large and thus modify considerably the size and mass of the complexes [7]. Detergent concentration affects protein self-association and function, through different mechanisms, particularly delipidation [8].

Analytical ultracentrifugation (AUC) is the classical method for determination of the molecular mass and size of solubilized proteins and still plays a leading role. It combines particle separation and analysis into a powerful technique for the determination, in a rigorous thermodynamic way, of the protein's size, mass, composition, and interactions [9–11]. Given recent developments in data analysis by P. Schuck and collaborators [12–14],

we investigate in this work the potential of sedimentation velocity (SV) to characterize detergent-solubilized membrane proteins: particularly the homogeneity, the amount of bound detergents, and the oligomeric structure. Two membrane proteins solubilized with DDM were studied: the sarcoplasmic reticulum Ca^{++}-ATPase and ExbB.

Ca^{++}-ATPase (SERCA1a), a P-type enzyme, is responsible for active calcium transport from the cytosol to the lumen of the sarcoplasmic reticulum. Rabbit SERCA1a can be considered as a model membrane protein due to its abundance in its native membrane, as well as to its stability after detergent solubilization [15]. The enzyme amounts to about 75% of the protein in the sarcoplamic reticulum, where it is by far the most abundant membrane protein. It has been well characterized biochemically and hydrodynamically. The size and state of aggregation in various detergents, the amount of bound detergents and lipids have been determined [16]. The pump is made of single polypeptide of about 110 kDa, with ten α-helical transmembrane segments and a large cytoplasmic head comprising about 2/3 of the protein [17]. In recent years, crystal structures that correspond to a number of pumping cycle intermediates have been obtained, which has produced a good description of the Ca^{++} transport process [18, 19].

ExdB is an accessory protein of TonB protein, which couples the electrochemical potential of the cytoplasmic membrane to active transport across the essentially unenergized outer membrane of gram-negative bacteria. In conjunction with another accessory protein ExbD, ExbB is required for both TonB energization and for recovering of TonB from the outer membrane after the energy transduction event [20]. ExbB is predicted to contain three membrane spanning segments starting with the N terminus in the periplasm and oriented with the largest part of the protein in the cytoplasm. In contrast, TonB and ExbD span the membrane only once with the bulk of the protein in the periplasm. Experimental evidence indicates that all three proteins act as a complex. ExbB interacts with ExbD and TonB, stabilizing both of them. The complementary topologies of ExbB and ExbD point towards their function as signal transducers with the soluble domains of each protein serving as interaction sites with other proteins. Even though ExbB and ExbD are encoded from a single operon and appear to function synergistically, ExbB exists in the cell at a 3.5 molar excess relative to ExbD. Stoichiometric analysis reveals a cellular ratio of 1 TonB/2 ExbD/7 ExbB, which suggests a complex of ~260 kDa [21]. In a crystallographic study of TonB, the protein appears as a dimer. It is not clear if this is a functional state, but if there are two TonB proteins per complex, there will be 4 to 5 ExbD and 14 to 15 ExbB proteins per complex, i.e., the entire complex would be ~520 kDa. The large excess of ExbB compared with the other proteins of the complex raises two possibilities: (1) simple ExbB/ExbD heterohexamers, or (2) ExbB multimers could alone constitute the proton translocator that energizes TonB. In the latter possibility, ExbD would participate with other ExbB multimers in recycling of TonB [22].

Ca^{++}-ATPase and ExbB were studied here in the presence of DDM, using SV protocols similar to those used for the characterization of detergent micelles [23]. These protocols were found suitable to determine the aggregation number and dimension of the DDM micelle from SV profiles. Reliable values for the partial specific volume were determined from complementary SV experiments in heavy water. The number of interference fringes corresponding to the micelles was also determined [23]. Even at low detergent concentration close to the CMC, the concentration of micelles in solution estimated with accuracy. In the present study, we now apply these procedures to the study of solubilized membrane protein complexes in order to quantify the amounts of bound and free detergent, thereby permitting the determination of the protein association states within these complexes.

2 Theoretical Background

For each homogeneous ideal solute, the sedimentation, i.e., the evolution of the weight concentration, c, with time, t, and radial position, r, is given by the Lamm equation:

$$(\partial c/\partial t) = -1/r\,\partial/\partial r\left[r(c\,s\,\omega^2 r - D\,\partial c/\partial r)\right], \tag{1}$$

ω being the angular velocity of the rotor in the centrifuge.

The sedimentation coefficient, s, and the diffusion coefficient, D, are related to the properties of the macromolecule: buoyant molar mass, M_b, and hydrodynamic radius, R_s, and to the solvent viscosity, η°. The Svedberg and the Stokes–Einstein relations are respectively:

$$RT\,s/D = M_b, \tag{2}$$

$$D = kT/6\pi\eta^\circ R_s, \tag{3}$$

$R = N_A k$ being the gas constant, N_A Avogradro's number, k Boltzmann's constant, T the temperature. M_b is related to the molar mass, M, and partial specific volume, $\bar{v}$, of the particle and to the solvent density, ρ°:

$$M_b = M(1 - \rho^\circ \bar{v}). \tag{4}$$

The Svedberg equation can also be written:

$$s = M_b/N_A 6\pi\eta^\circ R_s = M(1 - \rho^\circ \bar{v})/N_A 6\pi\eta R_s. \tag{5}$$

The frictional ratio f/f_{min} links the value of R_s to the minimum theoretical value, R_{min}, corresponding to the anhydrous volume of the particle:

$$R_s = f/f_{min} R_{min}. \tag{6}$$

For membrane proteins solubilized by detergents, M_b, M, and R_s are related to protein and amphiphile content. We use the indices PD for protein–detergent complex, P for protein, D for detergent, L for lipids. The Svedberg equation (5) relates the sedimentation coefficient s, buoyant molar mass M_{bPD}, and hydrodynamic radius R_s of the complex. M_{bPD} is related by Eq. 4 to the mass, M_{PD}, and partial specific volume, $\bar{v}_{PD}$, of the complex. If δ_D and δ_L are the amounts of bound detergent and lipids to the protein (in gram per gram) in the protein-detergent complex, M_{PD} and $\bar{v}_{PD}$ can be expressed as:

$$M_{PD} = M_P + \delta_D M_P + \delta_L M_P, \tag{7}$$

$$\bar{v}_{PD} = \left(\bar{v}_p + \delta_D \bar{v}_D + \delta_L \bar{v}_L\right)/(1 + \delta_D + \delta_L). \tag{8}$$

Moreover,

$$R_{min\,PD} = 3\pi \Big/ \left(4\left(N_A(M_P\bar{v}_P + \delta_D M_P \bar{v}_D + \delta_L M_P \bar{v} L)^{1/3}\right)\right). \tag{9}$$

M_{bPD} can be also expressed as:

$$M_{bPD} = M_P(1 - \rho^\circ \bar{v}_P) + \delta_D M_P(1 - \rho^\circ \bar{v}_D) + \delta_L M_P(1 - \rho^\circ \bar{v}_L). \tag{10}$$

The last lipid term of Eq. 10 is generally neglected in water since the density $1/\overline{v}_L$ of the lipids is often similar to the density ρ° of water: $\overline{v}_L$ values of 0.981 ml g^{-1} are indeed reported for egg yolk phosphatidylcholine and 0.93 ml g^{-1} for phosphatydylserine [11].

Experiments performed in D_2O solvents can provide $\overline{v}$ determination, if the macromolecule assembly (association state) and shape (R_s) are unaffected by isotopic substitution [1]. The Svedberg relation in the D_2O solvent, with the corresponding index D_2O, is:

$$s_{D20} = M_{bD20}/N_A 6\pi\ \eta^{\circ}_{D20} R_s. \tag{11}$$

If R_s does not change, R_{Mb}, the ratio of the buoyant molar masses, M_{bD20}, in D_2O, and M_{bH}, in H_2O solvents reduces to:

$$R_{Mb} = M_{bD20}/M_{bH} = s_{D20}\eta^{\circ}_{D20}/s\eta^{\circ}. \tag{12}$$

Because of the substitution of labile H for D, the mass of the particle increases to M_{D20} in the D_2O solvent, while isotopic substitution does not change its volume. As a consequence, the partial specific volume in D_2O can be expressed as a function of $\overline{v}$:$\overline{v}_{D20} = \overline{v}M/M_{D20}$, and, from Eq. 4:

$$M_{bD20} = M_{D20}\left(1 - (M/M_{D20})\rho^{\circ}_{D20}\overline{v}\right) = M\left((M_{D20}/M) - \rho^{\circ}_{D20}\overline{v}\right), \tag{13}$$

and $R_{Mb} = \left((M_{D20}/M) - \rho^{\circ}_{D20}\overline{v}\right)/(1 - \rho^{\circ}\overline{v})$, providing a relation which allows us to solve for $\overline{v}$ in terms of R_{Mb}:

$$\overline{v} = (M_{D20}/M - R_{Mb})/\left(\rho^{\circ}_{D20} - R_{Mb}\rho^{\circ}\right). \tag{14}$$

The closer to 1 is the value of $\overline{v}$, the more accurate its estimate from R_{Mb}. In addition, uncertainties on M_{D20}/M entail small errors on $\overline{v}$ for $\overline{v}$ close to 1 [1]. Corrected sedimentation coefficients at 20°C, $s_{20,w}$, in water (density ρ_{20w}=0.99828 g ml^{-1} and viscosity η_{20w}=1.002 mPa s) are obtained in the usual way for the data obtained in H_2O solvent:

$$s_{20,W} = (\eta^{\circ}/\eta_{20w}).((1 - \eta_{20W}\overline{v})/(1 - \rho^{\circ}\overline{v})). \tag{15}$$

For the data obtained in D_2O solvent, we can write:

$$s_{20,w} = \left(\eta^{\circ}_{D20}/\eta_{20W}\right).\left((1 - \eta_{20W}\overline{v})/(M_{D20}/M) - \rho^{\circ}_{D20}\overline{v})\right). \tag{16}$$

Determination of the Refractive Index Increments From Analytical Ultracentrifugation The number of fringes J of interference measured in the analytical ultracentrifuge is related to the refractive index increments $\partial n/\partial c$ (ml g^{-1}) and species concentration c (g ml^{-1}), according to:

$$(\partial n/\partial c) = (J/c)(\lambda/Kl), \tag{17}$$

with λ as the wavelength of the laser (675 10^{-7} cm in our experiments), K=1 the magnifying coefficient, and l the optical path of the cell (1.2 cm in our case). From Eq. 17,

a molar "extinction coefficient" of fringe number, ε_J, *i.e.* the number of fringe shift J for the sedimenting species at 1M and for 1 cm of path-length, can be expressed :

$$\varepsilon_J = (M/1000)\,(\partial n/\partial c)(K/\lambda)lc \tag{18}$$

The denominator 1,000 is related to the ml to l IU conversion.

Determination of the Amount of Bound Detergent to the Protein from Analytical Ultracentrifugation The dependence on the refractive index with the protein concentration, c_p, is given by the equation [24, 25]:

$$(\partial n/\partial_{CP})_{PD} = (\partial n/\partial_{CP})_P + (\partial n/\partial_{CD})_D \delta_{DL} \tag{19}$$

where $(\partial n/\partial c_P)_{PD}$ (ml g^{-1}) is the refractive index increment for the protein–detergent complex expressed in terms of protein concentration c_P, $(\partial n/\partial c_P)_P$ is the refractive index increment for the protein in terms of protein concentration c_P—for membrane proteins—$(\partial n/\partial c_D)_D$ is the refractive index increment for the detergent in terms of detergent concentration, c_D, and δ_{DL} is the amount of detergent and lipid bound to the protein in grams per grams. In this treatment, we consider that $\partial n/\partial c$ is the same for the detergent and lipids.

Effect of Pressure in the Ultracentrifuge The pressure change ΔP in the solvent at a radial position $(r-r_b)$, with r_b the meniscus position at atmospheric pressure P_{atm} is related to the solvent density, $\rho°$, and force field, $g_c=\omega^2 r$ in the ultracentrifuge:

$$\Delta P = \rho^\circ\, g_c(r - r_b) \tag{20}$$

if we consider the density of water: $\rho°=1$ g ml^{-1}, $(r-r_b)=1$ cm, and the maximum force field in a commercial ultracentrifuge of $g_c=300{,}000$ $g=300{,}000\times 9.8$ m s^{-2}, which corresponds to an angular velocity of 60,000 rpm and radial position of 7.2 cm. We obtain: $\Delta P=30\times 10^6$ Pascal=300 atm. The maximum value of g_c in our experimental conditions (42,000 rpm and 7.2 cm) is 140,000 g, corresponding to 140 atm. Application of pressure on solubilized membrane proteins may change detergent and protein properties since any equilibrium involving changes in the volume of the components may be affected. For example, the formation of hydrophobic contacts is accompanied by large positive volume changes due release of organized water molecules (hydrophobic hydration of apolar residues) [26]. Indeed, the CMC of cationic detergents in solution was shown to increase slightly (typically 10%) when increasing pressure up to 1,000 atm [27]. This is related to partial molal volume changes for micelle formation in the range 3–11 ml/mol [27]. In a previous work [23], we have characterized by SV the behavior in solutions of two detergents, DDM—which is used in this work—and octaethylene glycol monododecyl ether ($C_{12}E_8$). The values obtained of R_H, $\bar{v}$, agregation number, and CMC for these two detergents agree with values obtained by other techniques [7]. Nonetheless, the effect of pressure should be considered. In practice, a duplicate SV experiment run at two different angular velocities, e.g., 42,000 and 60,000, which correspond to pressures differing by a factor of two, will indicate if pressure effects are significant.

3 Materials and Methods

Buffers In the study of Ca^{++}-ATPase, "H_2O–TES medium" is 20 mM TES–NaOH, pH 7, 100 mM KCl, 0.5 mM $CaCl_2$, 1 mM $MgCl_2$. "H_2O–TES medium+ DDM" includes 1 mg ml^{-1}—i.e., 1.9 mM—dodecyl-β-D-maltoside (DDM); "D_2O–TES medium + DDM" contains D_2O instead of H_2O. In the study of ExbB, "H_2O–Tris medium" is 150 mM NaCl, 50 mM Tris, pH 8; "H_2O–Tris medium + DDM" includes 1.5–mg ml^{-1} DDM.

Samples Sample "Ca^{++}-ATPase 1" of solubilized delipidated Ca^{++}-ATPse was prepared according to the standard procedure [16], followed by gel filtration in "H_2O–TES medium+ DDM" [28]. Samples "Ca^{++}-ATPase 2" and "Ca^{++}-ATPase 3" were obtained by threefold dilution of "Ca^{++}-ATPase 1" in "H_2O–TES medium+ DDM" and "H_2O–TES medium", respectively. The sample "Ca^{++}-ATPase 1 in D_2O" was obtained after 14 h dialysis in "D_2O–TES medium + DDM".

Strain *E. coli* ER2566 (New England Biolabs, Beverly, MA) carrying a plasmid coding for C-terminally His-tagged ExbB (ExbB–His_6) was used to overexpress the recombinant protein. Bacteria bearing the plasmid were induced with 0.4 mM IPTG for 2 h at 37°C when the cultures reached an optical density of 0.8 at 600 nm. The cells were then collected by centrifugation, resuspended in lysis buffer (50 mM Tris, pH 8, 150 mM NaCl, 1 mM EDTA) and disrupted by three passages through a French pressure cell at 12,000 psi. All the steps were carried out at 4°C or on ice and the buffer supplemented with protease inhibitor cocktail tablets (Roche). Cell membranes were pelleted at 4°C (100,000×*g*, 50 min) and suspended in solubilization buffer (50 mM Tris, pH 8, 500 mM NaCl, 5 mM $MgCl_2$, 3% DDM). Soluble material was further purified using an FPLC (Amersham Pharmacia Biotech) in a two chromatographic steps protocol (Ni-Hitrap and HiTrapQ columns, Pharmacia) according to the manufacturer's instructions. Sample "ExbB 1" was obtained following ion-exchange chromatography in "H_2O–Tris medium + DDM" and concentrated three times to 1 mg ExbB per ml using Centricon 30 (Amicon) concentrators. Samples "ExbB 2" and "ExbB 3" were obtained by threefold dilution in "H_2O–Tris medium+ DDM" and "H_2O–Tris medium", respectively. From optical density measurements at 280 nm (A_{280}), the concentration of "Ca^{++}-ATPase 1" and "ExbB 1" were 1 mg ml^{-1}, of "Ca^{++}-ATPase 2", "Ca^{++}-ATPase 3," and "ExbB 2" were 0.34 mg ml^{-1} and of "ExbB 3" 0.4 mg ml^{-1}.

Numerical Values for Sedimentation Velocity Analysis Solvent densities, ρ, were measured with a DMA5000 density meter (Anton Paar, Graz, Austria) as 0.998, 1.004, 1.109 g ml^{-1}, for H_2O, "H_2O–TES medium", "D_2O–TES medium", respectively. Solvent viscosities, η, were measured with a AMVn viscosity meter (Anton Paar, Graz, Austria) as 0.981, 0.99, 1.00, and 1.23 mPa s for H_2O, "H_2O–TES medium", "H_2O–TES medium + DDM", and "D_2O–TES medium", with a precision of ~2%. For "H_2O–Tris medium," $\rho = 1.006$ g ml^{-1} and $\eta = 1.03$ mPa s were evaluated from tabulated data with the Sednterp program (available at http://www.jphilo.mailway.com/download.htm#SEDNTERP). Sednterp was also used to calculate, for Ca^{++}-ATPase and ExbB, values for the partial specific volumes at 20°C, $\bar{v}_P$, of 0.7425 and 0.743 ml g^{-1}, respectively, for the molar masses, M_P, values of 109,490 and 27,353 g mol^{-1}, respectively, for the molar extinction coefficient at 280 nm, ε_{280nm}, values of 105,800 and 20,910 $M^{-1}cm^{-1}$, corresponding to absorbance per mg ml^{-1}, $E_{0.1\%,280}$, of 0.966 and 0.764, respectively. We used, for the increments of refractive index $\partial n/\partial c$, values of

0.187 ml $g^{-1}$for the proteins [24], from which we derived ε_J values (molar "extinction" coefficient in fringe shift, see Eq. 18) of 303,259 and 75,777 $cm^{-1}M^{-1}$ for Ca^{++}-ATPase and ExbB, respectively. We consider M_D=511 Da, $\bar{v}_D = 0.82$ ml g^{-1} and $\partial n/\partial c$= 0.143 ml g^{-1} for the detergent DDM [23], ε_{280nm}=0, and ε_J=1,082.53 $cm^{-1}M^{-1}$. For the analysis of data obtained in D_2O solvent, we considered M_{D20}/M=1.015 in Eqs. 13, 14, and 16: the molar mass of proteins increases typically by a factor of 1.015 in 100 % D_2O [1]; for DDM, considering that seven H can be exchanged into D in deuterated solvents, the molar mass of DDM increases by a factor of 1.014 in 100 % D_2O.

Analytical Ultracentrifugation Experiments All experiments were conducted at 20°C. Sedimentation velocity (SV) experiments were performed on a Beckman Coulter XL-I analytical ultracentrifuge at a rotor speed of 42,000 rpm (the maximum rotor speed recommended for the centerpieces used). We used Al-Epon double sector 1.2 cm optical path centerpieces equipped with sapphire windows filled with, typically, 400 µl sample and 400 µl solvent reference without detergent: "H_2O–TES medium" or "H_2O–Tris medium". Sedimentation profiles were acquired overnight using absorbance at 280 nm and interference optics every 7 min.

SV Analysis Analyses were typically made considering a total of 16 h sedimentation. The programs used for data analysis, Sedfit version 8.9 and Sedphat (freely available at http://www.analyticalultracentrifugation.com) are described in detail on the web site. Briefly, Sedfit is used for the global analysis of one set of SV profiles from one experiment, while Sedphat can analyze globally several SV experiments. Sedphat also analyzes the data in terms of corrected sedimentation coefficients ($s_{20,w}$).

Continuous Distribution c(s) Analysis The $c(s)$ method [12, 13] deconvolutes the effects of diffusion broadening, producing a high-resolution sedimentation coefficient distribution. The program Sedfit does the calculation by assuming a relationship between the sedimentation and diffusion coefficients, through reasonable values of $\bar{v}$, of the frictional ratio f/f_{min}, of ρ°, and of the solvent viscosity η°. The analysis is based on finite element solutions of the Lamm equation (Eq. 1) and algebraically accounts for the systematic noise of the experimental data. The Lamm equation was simulated for 200 particles in the range (0.01 S, 20 S) for Ca^{++}-ATPase and (0.01 S, 6 S) for ExbB. We used, for the detergent-solubilized proteins, values of $\bar{v}$= 0.78 and 0.8 ml g^{-1} for Ca^{++}-ATPase and ExbB, respectively, i.e., intermediate between DDM and protein, f/f_{min}=1.25 (which corresponds to a globular, usually hydrated, particle), and the experimental values for ρ° and η°. All the $c(s)$ distributions were calculated without and with regularization procedure (confidence level of 0.7).

Analysis in Terms of Non-interacting Species This model evaluates, without any assumptions, for each species (up to 3), independent values of the sedimentation and diffusion coefficients, s and D (see Eq. 1). The program Sedphat allows the global analysis of SV experiments performed with different samples and/or optics. For each sample, the absorbance and fringe shift characterizing the different types of species are also obtained. The sedimentations of the three samples of detergent-solubilized ExbB were globally analyzed in terms of absorbance and interference data with a three non-interacting species model (detergent monomer, detergent micelle and protein–detergent complex). The model was not appropriate for the samples of detergent-solubilized Ca^{++}-ATPase which were slightly heterogeneous. In practice, Sedphat requires "a" value of $\bar{v}$ common to all species,

and provides the values of $s_{20,w}$ and M (calculated by the program from the experimental s and D with Eqs. 2 to 4 and input values of $\bar{v}$, $\rho°$ and $\eta°$). In the general case of PD complexes, i.e., systems with species with different $\bar{v}$, the hypothesis of a common $\bar{v}$ may be not appropriate: the output values of $s_{20,w}$ and M (M_{output}) for species may be inexact, and the experimental s and M_b need to be recalculated from $s_{20,w}$, M_{output} and the input value of $\bar{v}$ (for ExbB solutions, $\bar{v}_{input}$=0.8 ml g^{-1}). Since the conversion of s to $s_{20,w}$ depends essentially on $\eta°$ when $\rho°$ is close to the density $\rho°_{20w}$ of water at 20°C (which was the case), the values of $s_{20,w}$ can be accepted here. M_b is derived from M_{output} and $\bar{v}_{input}$: $M_b = {}_{output}(1-\rho°\bar{v}_{input})$. M can then be derived with Eq. 4. R_s is calculated from the output values of $s_{20,w}$ and M (or in a strictly equivalent way, from s and M_b).

Multiwavelength Analysis of Sedimentation Velocity Data This analysis takes advantage of the difference in the optical properties of the different components named "chromophores" of a multi-component mixture. It requires data acquired with different systems of detection (here, we have two wavelengths: A_{280} and interference, for two components: detergent + lipid—considered as one component—and protein). It determines $c_k(s_{20,w})$, the distributions of the corrected sedimentation coefficient $s_{20,w}$ expressed in μM for each of the components k in solution [14]. Theory and applications can be found at http://www.analyticalultracentrifugation.com/sedphat/multi-signal_c(s).htm. The user has to supply the relation between the signal and molar concentration for 1-cm path length for each signal ("extinction" coefficients ε_J and ε_{280nm}) for each "chromophore" (proteins and detergent). For our analysis, the Lamm equation was simulated for 200 particles in the range (1 S, 15 S) for Ca^{++}-ATPase and (1 S, 6 S) for ExbB. We also supplied $f/f°$=1.33 and $f/f°$=1.25 for Ca^{++}-ATPase and ExbB, respectively. We have used the option "unnormalized data": when the distribution are copied into an Excel file; the μM concentrations corresponding to each sedimentation particle (peak) are obtained by sum of the $c(s)$ in the appropriate s-range (selecting "normalized data" would have provided μM concentrations related to area under the curves). All the $c_k(s)$ distributions were calculated with the Tikhonov regularization procedure (confidence level of 0.7).

4 Results

Sedimentation Velocity of Ca^{++}-ATPase in "H_2O–TES medium + DDM": General Behavior Figure 1 shows the difference between sets of sedimentation profiles of Ca^{++}-ATPase in "H_2O–TES medium + DDM" obtained using different optics. Absorbance at 280 nm (Fig. 1a, A) displays a nice boundary corresponding to the Ca^{++}-ATPase–DDM complex. Interference (Fig. 1b, A) shows clearly an additional slower boundary, corresponding to the DDM micelles, which are not detected by absorbance optics.

Size distribution Analysis of Ca^{++}-ATPase in "H_2O–TES medium + DDM": Ca^{++}-ATPase 1 The sedimentation profiles are analyzed first in terms of particle distributions using the $c(s)$ analysis. The superimposition of the experimental and modeled sedimentation profiles are shown in Fig. 1a and b (A). The residuals are nearly randomly distributed around zero, indicating good fits (Fig. 1a and b, B). As shown on Fig. 1a and b (C) for "Ca^{++}-ATPase 1", the pattern of $c(s)$ is essentially the same above 4S with the two optics, with one main peak (62% of the total signal at 280 nm) attributed to the main Ca^{++}-ATPase–DDM complex at

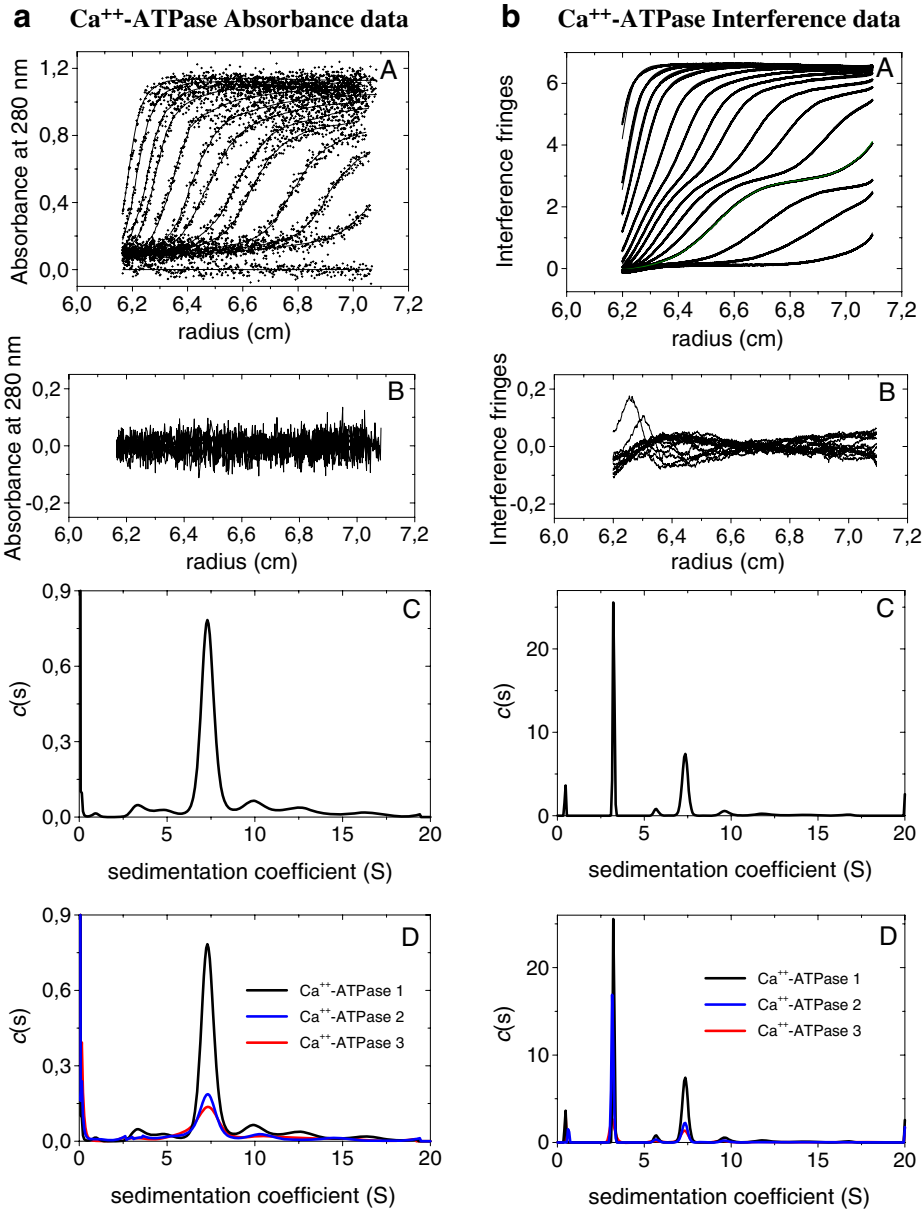

Fig. 1 Sedimentation velocity of Ca^{++}-ATPase in "H_2O–TES medium + DDM" from **a** absorbance data at 280 nm, and **b** interference data. *A* selection of experimental (*dots*) and fitted (*continuous line*) profiles corrected for all systematic noises, for the Ca^{++}-ATPase obtained from chromatographic column. The last profiles correspond to 8 h of sedimentation at 42,000 rpm at 20°C; *B* superposition of the difference between the experimental and fitted curves; *C* corresponding *c*(*s*) distribution; *D* superimposition of the *c*(*s*) distributions for Ca^{++}-ATPase obtained from size exclusion chromatography (Ca^{++}-ATPase 1), Ca^{++}-ATPase obtained from size exclusion chromatography and diluted three times with solvent containing DDM (Ca^{++}-ATPase 2) or with solvent without DDM (Ca^{++}-ATPase 3)

7.13 S ($s_{20,w}$=7.2 S). Other minor peaks are detected at larger s. They correspond most probably to aggregates of the protein–detergent complex. Interference shows, at 3.1 S ($s_{20,w}$=3.2 S), the DDM micelles, as it was the only peak for "H_2O–TES medium + DDM" solvent measured in the same conditions (not shown). The small contribution observed at 280 nm indicates absorbing impurities in the detergent micelles. Thus, the $c(s)$ analysis, an extremely powerful tool for the evaluation of sample homogeneity, shows the Ca^{++}-ATPase sample is slightly heterogeneous. Detergent micelles are easily distinguished from the protein complexes.

Protein and Detergent Concentration Effects for Ca^{++}-ATPase The concentration dependence of the sedimentation permits the evaluation of detergent-mediated association–dissociation processes. The comparison of the $c(s)$ analysis for "Ca^{++}-ATPase 1" with those of "Ca^{++}-ATPase 2" and "Ca^{++}-ATPase 3"corresponding to samples three times diluted with a solvent containing or not DDM, is shown in Fig. 1a and b (D) for data obtained at 280 nm and using interference optics, respectively. The sedimentation coefficient value for the main species does not depend on sample concentration (see also Table 1). The contribution of DDM at 3.1 S is clearly observed in the $c(s)$ obtained from interference data (Fig. 1b, D). The areas under the two major peaks of the two $c(s)$ distributions are reported in Table 1. They are related to DDM micelle concentration (DDM) and Ca^{++}-ATPase–DDM complex composition and concentration.

The Ca^{++}-ATPase–DDM complexes represent 62%, 53%, and 37% of the total of absorbance signal in the Ca^{++}-ATPase 1, 2, and 3, respectively. The sample's proportion of the major peak thus depends on the concentrations of the Ca^{++}-ATPase and DDM. Significantly, Ca^{++}-ATPase 3 contains aggregates in slightly larger amounts when DDM concentration is decreased from 1 to 0.3 mg ml^{-1}.

Amount of Bound Detergent of Ca^{++}-ATPase in "H_2O–TES medium + DDM" The nearly constant value $s_{20,w}$, 7.38±0.1 S, suggest that the main Ca^{++}-ATPase–DDM complex has always the same composition. For each sample, the area under this peak from absorbance data ($A_{280\ PD}$) and from interference (fringe shift J_{PD}) are reported on Table 1. The ratios $J_{PD}/A_{280\ PD}$ are nearly the same for the three samples (4.6, 4.4, and 5 for Ca^{++}-ATPase 1, 2, and 3, respectively), suggesting again the invariance in the complex composition. For each sample, the protein concentration c_P in g ml^{-1} was evaluated from $A_{280\ PD}$; the refractive index increments for the protein−detergent complex $(\partial n/\partial c_P)_{PD}$ (ml g^{-1}) was then calculated from c_P and J_{PD} using Eq. 17. Since the contribution $(\partial n/\partial c_D)_D$=0.143 is known [23], the amount of bound detergent to the protein (δ_D) for each sample was evaluated from $(\partial n/\partial c_P)_{PD}$ using Eq. 19. Lipids are not considered since Ca^{++}-ATPase is obtained in a delipidated form [16, 28]. We obtain for the three samples similar values of δ_D=0.93± 0.15 g/g. It is in the range of the values 0.75–0.9 g/g reported in the literature [16, 28].

Multiwavelength Analysis of Ca^{++}-ATPase in "H_2O–TES medium + DDM" The multi-signal $c_k(s)$ analysis was applied to the most concentrated sample, Ca^{++}-ATPase 1, in order to determine sedimentation coefficient distributions. We have considered that the detergent DDM and the protein Ca^{++}-ATPase are the only two chromophores of the mixture. Their characteristic ε_{280} and ε_J are given in Section 3 above. For clarity in the representation, we have considered DDM as assemblies of 100 monomers. The result of the analysis is presented in Fig. 2: A unit of 1 μM on the figure represents 1 μM of Ca^{++}-ATPase or 100 μM DDM.

Table 1 Values of parameters characterizing the Ca^{++}-ATPase –DDM complex

	A_{280} or J total	$A_{280\ PD}$ or J_{PD}	s_{PD} (S)	$s_{20,w,\ PD}$ (S)	$M_{b\ PD}$ (kDa)	M_{PD} (kDa)	c_P (mg ml^{-1})	$(dn/dc_P)_{PD}$ (ml g^{-1})	δ_{DL} (g/g)	s_{DDM} (S)	$s_{20,w}$ (S)	J_{DDM} (J)
Ca^{++}-ATPase 1												
Abs. 280 nm	1.06	0.66	7.13	7.28	45	206	0.57					
Interference	7.04	3.03	7.13	7.28	45	206		0.30	0.9	3.07	3.10	3.09
Ca^{++}-ATPase 2												
Abs. 280 nm	0.39	0.21	7.24	7.40	46	209	0.18					
Interference	4.14	0.92	7.33	7.50	47	210		0.29	0.8	3.17	3.20	2.57
Ca^{++}-ATPase 3												
Abs. 280 nm	0.4	0.15	7.18	7.34	45	207	0.13					
Interference	2.48	0.75	7.30	7.47	46	210		0.33	1.1	3.18	3.20	0.85
Mean Values			7.22±0.1	7.38±0.1	46±1	208±2			0.93±0.15			
Ca^{++}-ATPase 1 in D_2O												
Abs. 280 nm	1.13	0.57	4.10	8.20	31	230	0.57					
Interference	10.8	2.61	4.10	8.20	31	230		0.3	0.9	1.50	3.60	2.80

Values for signal are given for 12 mm path length; PD refers to Ca^{++}-ATPase–DDM complex at 7.1S; $s_{20,w}$ were calculated with $\bar{v}_{PD}$= 0.78 ml g^{-1} and $\bar{v}_D$= 0.82 ml g^{-1}; $M_{b\ PD}$ is calculated with Eqs. 2 and 3 from s and R_s=55 Å measured in a previous work [26]; M_{PD} is obtained using $\bar{v}_{PD}$= 0.78 ml g^{-1} in Eq 4. In D_2O, $s_{20,w,\ PD}$ and M_{PD} are derived considering M_{D20}/M=1.015 in Eqs. 16 and 13. The concentration c_P of Ca^{++}-ATPase is from $A_{280\ PD}$ and used to derive $(\partial n/\partial c_P)_{PD}$ from J_{PD} with Eq. 17

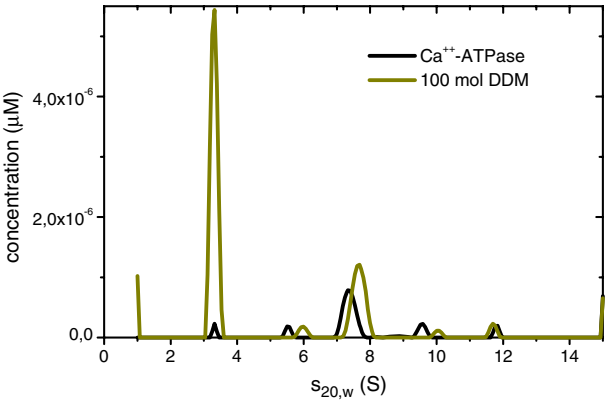

Fig. 2 Multiwavelength analysis of Ca^{++}-ATPase in "H_2O–TES medium + DDM" (Ca^{++}-ATPase 1)

This representation shows the species at nearly the same position as in the raw $c(s)$ distributions (Fig. 1). The "protein" and "DDM" distributions are essentially the same. The slight differences in the s-positions for the main peak do not have to be considered, as these are most probably due to the general approximation of the $c(s)$ analysis (same partial specific volume and frictional ratio) and to the different noise levels in the absorbance and interference data. The contributions of the smaller and larger aggregates are clearly distinct from that of the main species. The main contribution of DDM is at s_{20w}=3.3 S, i.e., in the DDM micelles. The main contribution of Ca^{++}-ATPase is found at s_{20w}=7.7 S and co-migrates logically with DDM. Table 2 reports the concentration of DDM and Ca^{++}-ATPase calculated from the analysis of these two peaks. The small amount of "Ca^{++}-ATPase" in the DDM micelles reflects some absorbing impurity. The main complex of Ca^{++}-ATPase–DDM corresponds to concentrations of 5.3 μM Ca^{++}-ATPase and 849 μM monomeric DDM, i.e., a molar ratio of 161 monomers of DDM per monomer of Ca^{++}-ATPase, corresponding to a ratio, δ_D, of 0.75 g DDM per gram protein. This value is close to the value of 0.93 g/g determined above from the independent analysis the SV experiments obtained at 280 nm and by interference and is in the range reported in the literature [16, 28].

Association State of Ca^{++}-ATPase in the Main Complex from s and R_s, and Composition
The combination of the s value determined for the main complex and of R_s=55 Å [28] gives a buoyant molar mass for the complex of M_{bPD}=46 kDa. Neglecting the eventual lipid contribution and considering the complex as a monomer, Eq. 10 gives very similar values with M_{bPD} of 42 or 45 kDa, for δ_D of 0.75 or 0.9 g/g, respectively. The possibility of a dimer

Table 2 Multiwavelength analysis of the samples of Ca^{++}-ATPase and ExbB

	Concentration (μM) detergent/protein ratio			
	Protein	Detergent	mol/mol	g/g
Ca^{++}-ATPase				
Micelle of DDM	0.42	2149	5117	24
Ca^{++}-ATPase–DDM complex	5.3	849	161	0.75
ExbB				
Micelle of DDM	11.4	5300	465	9
ExbB–DDM complex	25.5	2010	80	1.5

is furthermore excluded, since such case would result in M_{bPD} of 84 and 90 kDa, about twice the experimental M_{bPD}.

The molar mass M_{PD} is 208 kDa, from M_{bPD}=46 kDa and $\bar{\nu}_{PD}$= 0.78 ml g^{-1} (the calculated value for the complex for δ_D of 0.75 or 0.9 g/g; Table 1). It is about twice the value of the monomeric Ca^{++}-ATPase (M=109 kDa), which is expected since there is approximately 1 g of bound detergent per gram protein.

Comparison of the Sedimentation Velocity of Ca^{++}-ATPase in "D_2O–TES Medium + DDM" and "H_2O–TES medium + DDM" The $c(s)$ distribution of Ca^{++}-ATPase 1 in D_2O from absorbance data gives one main peak attributed to the main Ca^{++}-ATPase–DDM complex (50% of the total signal) at 4.1 S ($s_{20,w}$=8.2 S, with $\bar{\nu}_{PD}$= 0.78 ml g^{-1}). There are also, as in the hydrogenated solvent, small contributions related to impurities or aggregates. Interference optics shows the DDM micelles at 1.5 S ($s_{20,w}$=3.6 S with $\bar{\nu}_D$= 0.82 ml g^{-1}). Combining the s value of the main PD complex with R_s=5 Å measured in [28] and δ_D= 0.75 or 0.9 g/g gives a molar mass of 230 kDa corresponding to the monomer associated with ~1 g of detergent per g of protein. From the analysis of the area under the PD peak, reported in Table 1, we found also a value for the amount of bound detergent δ_D=0.9 g/g, again similar to that found in the hydrogenated solvent.

From the values of the sedimentation coefficients in the two solvents, we calculate R_{Mb}= 0.707 using Eq. 12. Considering M_{D2O}/M=1.015, we derive a value for the partial specific volume $\bar{\nu}_{PD}$= 0.77 ml g^{-1}. This value is less than 0.01 ml g^{-1} that calculated for a complex with 0.75 to 0.95 g of DDM per g of protein. The s_H/s_D method thus provides a $\bar{\nu}_{PD}$ value in very good agreement with independent measurements of bound detergent (this work and [16, 28]).

Sedimentation Velocity of ExbB in "H_2O–Tris medium + DDM": General Behavior and Size Distribution Analysis Contrary to Ca^{++}-ATPase, the raw SV profiles obtained for ExbB at 280 nm and with interference are not obviously different [Fig. 3a and b (A)]. But good fits (Fig. 3a and b, B) with the $c(s)$ analysis reveal at 280 nm only one peak (ExbB–DDM complex) at 3.6 S ($s_{20,w}$=3.8 S) and, with interference, the additional presence of DDM micelles at 3 S ($s_{20,w}$=3.1 S).

Figure 3a and b (D) show the superimposition of the $c(s)$ distributions from A_{280} and interference data, respectively, for the stock sample of ExbB and the same sample diluted three times with solvent with or without DDM (1.5 mg ml^{-1}, 3 mM). All $c(s)$ from 280 nm show only one peak at ~3.6 S but differ in area, i.e., ExbB concentration. All the $c(s)$ distributions from interference (Fig. 3b, D) show only two peaks attributed to the DDM micelles at ~3 S and ExbB–DDM complex at ~3.6 S. Because of the invariance in the position of the two peaks in the $c(s)$, we analyzed our data in terms of two non-interacting species.

Global Analysis of ExbB in "H_2O–Tris medium + DDM" in Terms of Non-interacting Species The six sets of SV profiles (three samples observed with absorbance and interference) were analyzed globally with a model for three non-interacting species (detergent monomer, micelle of detergent, and ExbB–detergent complex), using the program Sedphat. The fits are shown in Fig. 4 and the results given in Tables 3 and 4. For the detergent monomer (the molar mass of which was fixed to 511 Da), we found $s_{20,w}$= 0.1 S, for the micelle of DDM $s_{20,w}$=3.1 S and M=56 kDa (calculated with $\bar{\nu}_D$= 0.82 ml g^{-1}), and for the ExbB–DDM complex $s_{20,w}$=4 S, M=77 kDa (using $\bar{\nu}$= 0.8 ml g^{-1}) and R_s=34 Å.

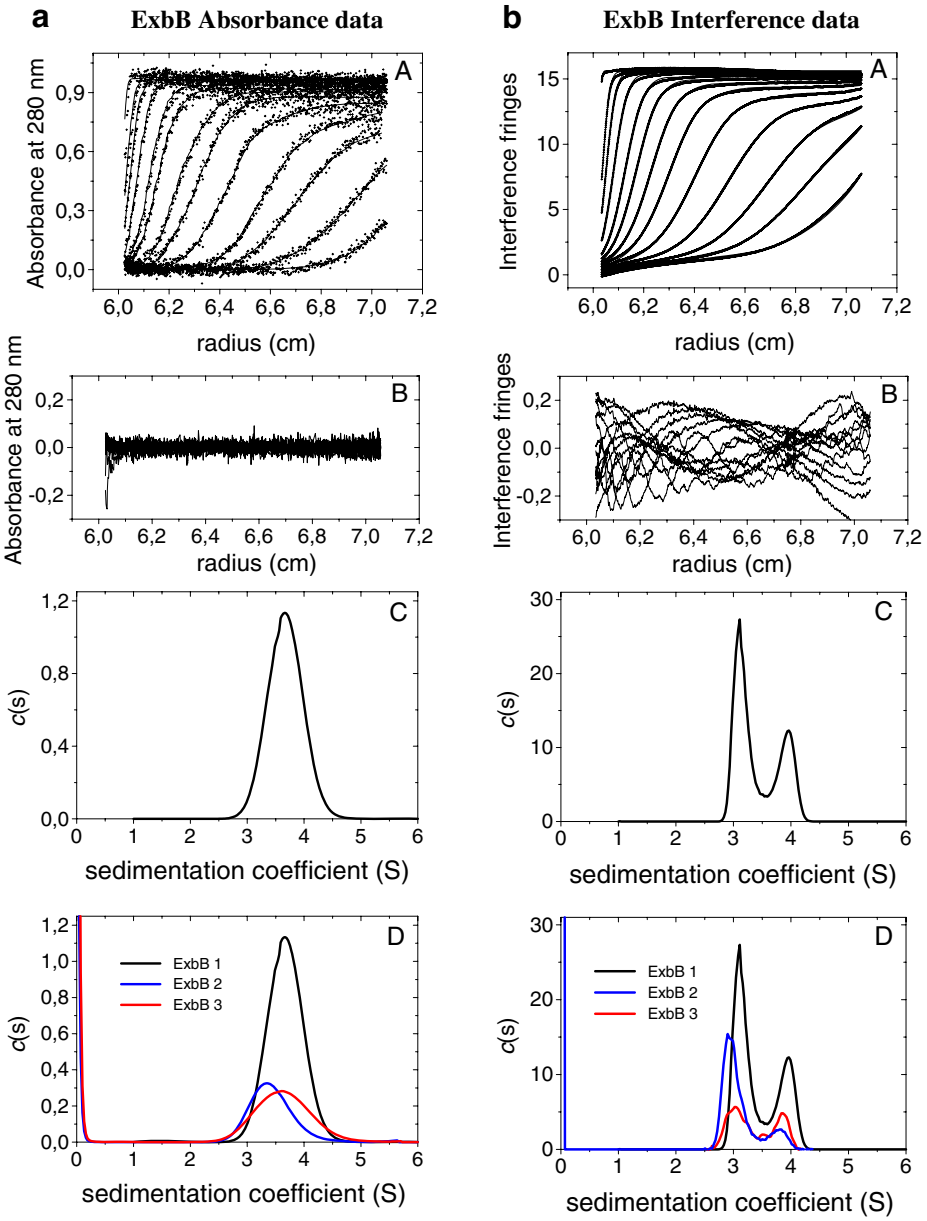

Fig. 3 Sedimentation velocity of ExbB in "H_2O–Tris medium + DDM" from **a** absorbance data at 280 nm, and **b** interference data. *A* selection of experimental (*dots*) and fitted (*continuous line*) profiles corrected for all systematic noises, for ExbB obtained from chromatographic column. The last profiles correspond to 8 h of sedimentation at 42,000 rpm et 20°C; *B* superposition of the difference between the experimental and fitted curves. Note the maximum residual in **b** (*B*) is less than 2% the total number of fringes; *C* corresponding *c*(*s*) distribution; *D* superimposition of the *c*(*s*) distributions for ExbB obtained from chromatographic column and concentrated by ultrafiltration (ExbB 1), ExbB then diluted three times with solvent with DDM (ExbB 2) or without DDM (ExbB 3)

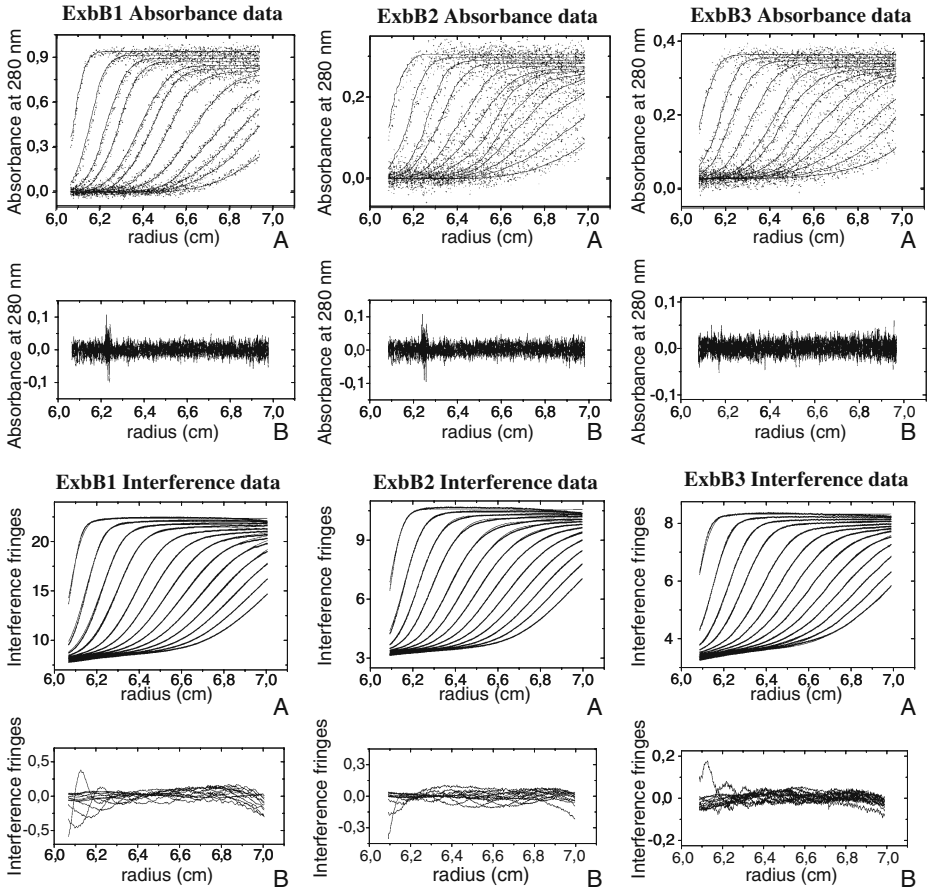

Fig. 4 Global analysis of the sedimentation of ExbB samples in terms of three non-interacting species: monomer of DDM, micelles of DDM, and ExbB–DDM complex. *A* The experimental (*dots*) and fitted data (*continuous line*) corrected for all systematic noises. The last profiles correspond to 8 h of sedimentation at 42,000 rpm; *B* the superimposition of the difference between the experimental and fitted curves

The analysis also provides for each SV experiment the absorbance signal A_{280} and the numbers of interference fringes J corresponding to ExbB complex (PD) or DDM (D) -see Tables 3 and 4. Comparison between the total J and A_{280} corresponds to the expected dilution factor. From J_D, the concentration of free detergent micelle can be estimated. It is much larger in a concentrated ExbB1 sample (2.6 mg ml^{-1}) than after elution from the gel filtration column (1.7 mg ml^{-1}). This indicates that the concentration step has significantly

Table 3 Global parameters for the ExbB–DDM complex and micelles of DDM; global analysis of the sedimentation of three ExbB samples solubilized in DDM

	s (S)	s_{20w} (S)	M_b (kDa)	M (kDa)	R_s (Å)
ExbB–DDM complex	3.8	4.0	15	77	34
Micelles of DDM	3.0	3.1	10	56	28

s_{20w} and M values are calculated using, for the ExbB–DDM complex, $\bar{v}_{PD}$= 0.8 ml g^{-1}, and, for DDM, $\bar{v}_D$= 0.82 ml g^{-1}

Table 4 Local parameters for the ExbB–DDM complex and micelles of DDM

	Interference signal J			Absorbance signal A						
	J_{PD}	J_D	c_D (mg ml^{-1})	A_{PD}	A_D	c_P (mg ml^{-1})	J_{PD}/c_P (ml mg^{-1})	$(dn/dc_P)_{PD}$ (ml g^{-1})	δ_{DL} *(g/g)*	δ_{DL} *(mol/mol)*
ExbB 1	7.1	6.7	2.6	0.82	0.14	0.90	7.8	0.44	1.76	94
ExbB 2	1.7	5.5	2.2	0.22	0.09	0.24	7.0	0.40	1.49	80
ExbB 3	1.9	2.8	1.1	0.26	0.08	0.28	6.7	0.38	1.35	72
3 mM DDM		4.3	1.7							

increased not only protein, but also detergent micelle concentration. We note also that although the micelles absorb at 280 nm, their absorbance decreases with dilution. This may reflect the presence in the concentrated sample of ExbB of small absorbing impurities that are dissolved in the detergent micelles (DDM by itself does not absorb). From the values of A_{280PD}, we calculate the concentrations of ExbB samples. The values of J_{PD}/c_P reported in Tables 3 and 4 show a mean value of 7.2 ml mg^{-1}. This value corresponds to $(\partial n/\partial c_P)_{PD}$= 0.41 ml g^{-1} for the ExbB–DDM complex and allows the amount of bound detergent and lipids to the protein to be estimated at δ_{DL}=1.53 g/g (Eqs. 17 and 19). We can therefore hypothesize that the absorbance of the ExbB–DDM complex is mainly related to protein content.

Multiwavelength Analysis of ExbB in "H_2O–Tris Medium + DDM" The multi-signal $c_k(s)$ analysis was used for the sample ExbB1 considering that the detergent DDM and the protein ExbB are the two chromophores of the mixture. The result of the analysis is represented in Fig. 5. ExbB and DDM are here found as components of the two particles sedimenting at $s_{20,w}$ of 3.3 and 4.2 S, corresponding to micelle DDM (with absorbing impurities) and PD complex. Results in terms of molar composition are given in Table 2. For the ExbB complex, 80 monomers of DDM are associated per monomer of ExbB or δ_{DL}=1.5 g/g (similar to δ_{DL}=1.53 g/g determined by the independent analysis of the $c(s)$ from A_{280} and interference). This estimate is dependent on the choice of extinction coefficient. Although DDM does not absorb by itself, which is true for pure DDM, the presence of absorbing impurities related to the purification process may have led, in our case, to a poor estimate of the protein content (and thus of bound DDM). We however

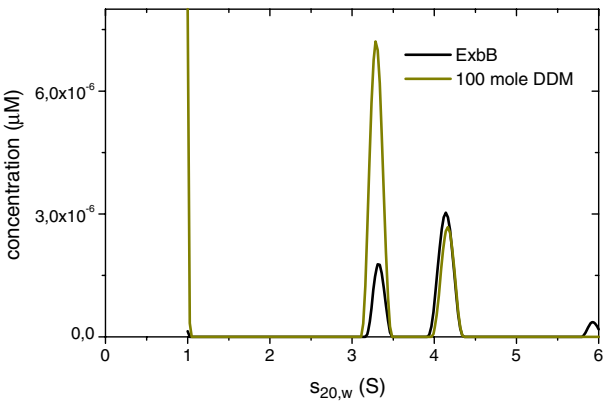

Fig. 5 Multiwavelength analysis of ExbB in "H_2O–Tris medium + DDM" (ExbB 1)

observe that the ratio of fringe number to absorbance (as reflected by the values of J_{PD}/c_P in Table 4) is the same for ExbB 2 and ExbB 3 (corresponding to samples diluted in buffers with and without detergent). Comparison of different samples is therefore crucial for the determination of complex composition.

Determination of the Association of ExbB in "H_2O–TES medium + DDM" From δ_{DL}= 1.5 g/g obtained from $c(s)$ or $c_k(s)$ analysis, we calculate M_{bPD} of 14.1 kDa if ExbB is a monomer, and 28.2 Da if it is a dimer (we have considered for bound detergent and lipid the value $\overline{v}_D$ for DDM of 0.82 ml g^{-1} providing $\overline{v}_{PD}$= 0.79 ml g^{-1}). The analysis in terms of two non-interacting species estimates s and D gives a buoyant molar mass for the complex M_{bPD} of 15 kDa, thus only compatible with a monomer. Furthermore, the analysis in terms of non-interacting species provides a hydrodynamic radius of 34 Å for the complex that corresponds to a monomer ExbB associated with DDM at 1.5 g/g to a frictional ratio of 1.22. It indicates a globular compact particle, which is a very plausible shape for a small detergent-solubilized protein. On the other hand, for a dimer of same composition, the s_{20w} value of 4S would lead to R_s=65 Å and f/f_{min}=1.8, i.e., a very extended and improbable shape.

All these arguments indicate that the sample of ExbB studied here was a monomer.

5 Conclusions

Analysis of SV experiments using numerical solutions of the Lamm equation have considerably increased the usefulness of the technique. We have recently shown that SV analysis adequately describes the hydrodynamic behavior of detergent solutions [23]. The present work explores the potential of SV analysis for membrane proteins. Solutions of detergent-solubilized membrane proteins are necessarily complex since they contain a minimum of three types of particles (detergent monomers, detergent micelles and protein–detergent complexes). This study is based on two examples, Ca^{++}-ATPase and ExbB. The former is well characterized; the association state of the latter had to be addressed as part of the present study.

Particle size distribution analysis, $c(s)$, allowed us to characterize the homogeneity of the samples. Ca^{++}-ATPase was found to be slightly heterogeneous, containing small amounts of aggregation in addition to the main complex, a result that is in agreement with former data [28, 29]. ExbB was found to be homogeneous with only one type of complex. DDM micelles (s_{20w}=3.1 S) and Ca^{++}-ATPase (s_{20w}=7.3 S) or ExbB (s_{20w}= 4 S) are clearly distinguished. Our typical protocol uses three samples; two of them are dilutions of the other with solvent with and without detergent. In each case, the final detergent concentration remained above the CMC. For Ca^{++}-ATPase, as for ExbB, analysis of the three samples shows only variation in the proportion of the species expected from dilution—except for a slight increase of the number of aggregates for Ca^{++}-ATPase at low detergent. There is no variation in the values of the sedimentation coefficients as a function of the detergent and protein concentrations, as was seen, for example, for detergent-solubilized HuPON-1 [4]. Ca^{++}-ATPase and ExbB, thus, do not show any evidence of equilibrium self-association (the only exception is a limited amount of aggregation at reduced detergent concentration; Fig. 1).

The combination of the $c(s)$ analysis of absorbance and interference data allows the estimation of bound detergent. Values of 0.93±0.15 g/g for Ca^{++}-ATPase are similar to the

values of 0.75 and 0.93 g/g, previously reported [16, 28]. For ExbB, we determined a value of 1.5 g/g for bound lipids and DDM. SV analysis in one solvent density condition cannot really discriminate between detergent and lipids. We thus combined their contribution as a pseudo-detergent one. This approach is valid, but the limits had to be evaluated. This determination is based on the J/A ratio (J is the number of fringes and A the absorbance), which can be obtained within the $c(s)$ analysis, i.e., for each type of particle that sediments at a different velocity in the ultracentrifuge. Thus, complexes from even heterogeneous samples can be analyzed properly. We tested the possibility of the deconvolution of the two sets of SV profiles using absorbance and interference in terms of component distribution (multiwavelength analysis [14]). From the relationships between concentration c and A and between c and J (true or pseudo-extinction coefficients) for detergent and protein, a representation of the data displaying the sedimentation of detergent and protein components can be obtained. For Ca^{++}-ATPase as for ExbB, the representation shows the expected co-sedimentation of the two components for the different particles: main complex, aggregates (if any) and also micelles (which incorporate absorbing impurities). It can thus allow determination of the stoichiometry of the different complexes. This type of analysis is of potential interest for the study of different detergent–protein assemblies in interaction. In particular, the programme Sedphat allows the fit of the extinction coefficient of an absorbing detergent (although this analysis was not used here since pure DDM does not absorb). The particle composition is also related to the value of the partial specific volume of the complex. It was estimated for Ca^{++}-ATPase as 0.77 ml g^{-1} by the combination of SV experiments in hydrogenated and deuterated solvents (i.e., differing in density). This value is the same as that calculated based on the determined composition. The value of the partial specific volume of the complex is required to convert the experimentally determined buoyant molar mass, M_b, into a molar mass, M, thus ascertaining the association state of the protein within the complex. M_b was obtained in different ways.

For Ca^{++}-ATPase, we combined the s value with the hydrodynamic radius, R_s, from complementary calibrated SEC [28]. The resulting value of M_b is only compatible with a monomer, which is expected [16]. For ExbB, the SV profiles can be analyzed in terms of non-interacting species (because the solution contains only two types of macromolecular assemblies) leading to the estimate of the diffusion coefficients, D, and thus R_s, in addition to s. The SV experiment by itself allows one to determine the association state of the membrane protein: In our samples, ExbB is a monomer. Previously reported, TonB complex stoichiometric analysis predicts a high number of ExbB within the complex (from 7 to 15, depending on the oligomerization state of TonB). The monomeric state of ExbB that we find in our experiments could be due to dissociation after the concentration step, which leads to high detergent concentration.

It is interesting to note that Ca^{++}-ATPase can be reconstituted into liposomes with a large excess of lipids. Under these conditions, it is possible to demonstrate that the protein is monomeric and transports Ca^{++} [30]. After solubilization in some detergents at appropriate detergent and protein concentrations, monomeric Ca^{++}-ATPase can be active (Ca^{++}-dependent ATPase activity [28]). Conversely, at low protein/detergent ratio, high protein concentration, in the presence of added lipid, or with some inefficient detergents, Ca^{++}-ATPase has a tendency to aggregate [7, 15, 29, 31]. It is of utmost importance to use robust techniques to test the aggregation state of detergent-solubilized membrane proteins.

Thus, by itself or in association with complementary techniques, SV offers the possibility to characterize in a rigorous way the composition and interactions of detergent-solubilized membrane protein complexes. One of the main advantages versus other techniques (such as scattering techniques or sedimentation equilibrium) is the possibility to control the

homogeneity of the samples, and to focus on a given complex even in the presence of other impurities or aggregates. This offers the possibility to control the association state of a membrane protein in a diversity of environments, for example, during the purification steps. Determining the amount of free detergent and how it affects macromolecular assemblies also can be highly useful in order to determine the association scheme and resolve multiple co-existing complexes [4–6]. The relative rapidity of SV measurements also allows working with unstable samples.

Sedimentation velocity-AUC appears as a method allowing the distinction between protein/detergent micelles (in their different association states), free detergent micelle, and detergent monomers. In one of our experiments, detergent DDM is detected as absorbing, which we interpret as contamination by absorbing material (most probably small hydrophobic material). This information may be an interesting feature in a quality control of membrane protein samples as the impurity may affect protein stability. In conclusion, the method offers a tool for characterizing membrane proteins and the potential, for example, for crystallization.

Acknowledgment The authors thank Prof. Lucienne Letellier for her support and helpful discussion. The authors are very grateful to Professor Neal C. Robinson and Dr. Nathan Zaccai for his critical reading of the manuscript. A.G.S. was supported by a CNRS fellowship (poste rouge). M.S. was recipient of a European Marie Curie Fellowship. C.E. and MlM thank the CEA DSV for a grant to develop the study of detergent-solubilized membrane proteins.

References

1. Gohon, Y., Pavlov, G., Timmins, P., Tribet, C., Popot, J.-L., Ebel, C.: Partial specific volume and solvent interactions of amphipol A8-35. Anal. Biochem. **334**(2), 318–334 (2004)
2. Lebaupain, F., Salvay, A.G., Olivier, B., Durand, G., Fabiano, A.-S., Michel, N., Popot, J.-L., Ebel, C., Breyton, C., Pucci, B.: Lactobionamide surfactants with hydrogenated, perfluorinated or hemifluorinated tails: physical–chemical and biochemical characterization. Langmuir **22**(21), 8881–8890 (2006)
3. Musatov, A., Robinson, N.C.: Cholate-induced dimerization of detergent—or phospholipid—solubilized bovine cytochrome C oxidase. Biochemistry **41**(13), 4371–4376 (2002)
4. Josse, D., Ebel, C., Stroebel, D., Fontaine, A., Borges, F., Echalier, A., Baud, D., Renault, F., le Maire, M., Chabrieres, E. Masson, P.: Oligomeric states of the detergent-solubilized human serum paraoxonase (PON1). J. Biol. Chem. **277**, 33386–33397 (2002)
5. Fleming, K.G.: Standardizing the free energy change of transmembrane helix–helix interactions. J. Mol. Biol. **323**, 563–571 (2002)
6. Fisher, L.E., Engelman, D.M., Sturgis, J.N.: Effect of detergents on the association of the glycophorin A transmembrane helix. Biophys. J. **85**, 3097–3105 (2003)
7. le Maire, M., Champeil, P., Møller, J.V.: Interaction of membrane proteins and lipids with solubilizing detergents. Biochim. Biophys. Acta Reviews on Biomembranes **1508**, 86–111 (2000)
8. Breyton, C., Tribet, C., Olive, J., Dubacq, J.-P., Popot, J.-L.: Dimer to monomer conversion of the cytochrome b6 f complex. Causes and consequences. J. Biol. Chem. **272**, 21892–21900 (1997)
9. Ebel, C.: Analytical Ultracentrifugation for the study of biological macromolecules. Progr. Colloid Polym. Sci. **127**, 73–82 (2004)
10. Ebel, C.: Analytical ultracentrifugation: State of the art and perspectives. In: Uversky, V., Permyakov, E.A. (eds.) Protein Structures: Methods in Protein Structure and Stability Analysis. Nova Science Publishers, New York (2007)
11. Ebel, C., Møller, J.V., le Maire, M.: Analytical ultracentrifugation: membrane protein assemblies in the presence of detergent. In: Pebay-Peyroula, E. (ed.) Biophysical approaches of structure and functions of membrane proteins. Wiley (2007)

12. Schuck, P.: Size-distribution analysis of macromolecules by sedimentation velocity ultracentrifugation and Lamm equation modelling. Biophys. J. **78**, 1606–1619 (2000)
13. Dam, J., Schuck, P.: Calculating sedimentation coefficient distributions by direct modeling of sedimentation velocity concentration profiles. Methods Enzymol. **384**, 185–212 (2004)
14. Balbo, A., Minor, K.H., Velikovsky, C.A., Mariuzza, R.A., Peterson, C.B., Schuck, P.: Studying multi-protein complexes by multi-signal sedimentation velocity analytical ultracentrifugation. PNAS **102**, 81–86 (2005)
15. Lund, S., Orlowski, S., de Foresta, B., Champeil, P., le Maire, M., Møller, J.V.: Detergent structure and associated lipid as determinants in the stabilization of solubilized Ca^{2+}-ATPase from sarcoplasmic reticulum. J. Biol. Chem. **264**, 4907–4915 (1989)
16. Møller, J.V., le Maire, M.: Detergent binding as a measure of hydrophobic surface area of integral membrane proteins. J. Biol. Chem. **268**(25), 18659–18672 (1993)
17. Møller, J.V., Juul, B., le Maire, M.: Structural organization, ion transport, and energy transduction of P-type ATPases. Biochim. Biophys. Acta **1286**, 1–51 (1996)
18. Toyoshima, C., Inesi, G.: Structural basis of ion pumping by Ca^{2+}-ATPase of the sarcoplasmic reticulum. Annu. Rev. Biochem. **73**, 269–92 (2004)
19. Møller, J.V., Nissen, P., Sørensen, T. L.-M., le Maire, M.: Transport mechanism of the sarcoplasmic reticulum Ca^{2+}-ATPase pump. Curr. Opin. Struct. Biol. **15**, 387–393 (2005)
20. Postle, K., Kadner, R.J.: Touch and go: tying TonB to transport. Mol. Microbiol. **49**(4), 869–882 (2003)
21. Higgs, P.I., Larsen, R.A., Postle, K.: Quantification of known components of the Escherichia coli TonB energy transduction system: TonB, ExbB, ExbD and FepA. Mol. Microbiol. **44**(1), 271–281 (2002)
22. Held, K.G., Postle, K.: ExbB and ExbD do not function independently in TonB-dependent energy transduction. J. Bacteriol. **184**, 5170–5173 (2002)
23. Salvay, A.G., Ebel, C.: Analytical ultracentrifuge for the characterization of detergent in solution. Progr. Colloid Polym. Sci. **131**, 74–82 (2006)
24. Hayashi, Y., Matsui, H., Takagi, T.: Membrane protein molecular weight determined by low-angle laser light-scattering photometry coupled with high-performance gel chromatography. Methods Enzymol. **172**, 514–525 (1989)
25. Yernool, D., Boudker, O., Folta-Stogniew, E., Gouaux, E.: Trimeric subunit stoichiometry of the Glutamate Transporters from Bacillus caldotenax and bacillus stearothermophilus. Biochemistry **42**, 12981–12988 (2003)
26. Masson, P., Balny, C.: Linear and non-linear pressure dependence of enzyme catalytic parameters. Biochim. Biophys. Acta **1724**, 440–450 (2005)
27. Osugi, J., Sato, M., Ifuki, N.: Micelle formation of cationic detergent solution at high pressures. The Review of Physical Chemistry of Japan **35**(1), 32–37 (1965)
28. Champeil, P., Menguy, T., Tribet, C., Popot, J.-L., le Maire, M.: Interaction of amphipols with sarcoplasmic reticulum Ca^{2+}-ATPase. J. Biol. Chem. **275**(25), 18623–18637 (2000)
29. le Maire, M., Møller, J.V., Menguy, T., Velours, J., Champeil, P.: Protein–protein contacts in solubilized membrane proteins, as detected by cross-linking. Anal. Biochem. **362**, 168–171 (2007)
30. Heegaard, C.W., le Maire, M., Gulik-Krzywicki, T., Møller, J.V.: Monomeric state and Ca^{2+}-ATPase, reconstituted with an excess of phospholipid. J. Biol. Chem. **265**, 12020–12028 (1990)
31. Chabre, M., le Maire, M.: Monomeric G-protein-coupled-receptor as a functional unit. Biochemistry **44**, 9395–9403 (2005)